

Electronic supplementary material:

Unveiling the Ir single atoms as selective active species for the partial hydrogenation of butadiene by *operando* XAS

W. Liu¹, F. Morfin², K. Provost¹, M. Bahri³, W. Baaziz³, O. Ersen³, L. Piccolo², C. Zlotea^{1*}

¹ *Université Paris Est, Institut de Chimie et des Matériaux Paris-Est (UMR7182), CNRS, UPEC, 2-8 rue Henri Dunant, 94320 Thiais, France*

² *Univ Lyon, Université Claude Bernard - Lyon 1, CNRS, IRCELYON - UMR 5256, 2 Avenue Albert Einstein, F-69626 VILLEURBANNE CEDEX, France*

³ *Université de Strasbourg, Institut de Physique et Chimie des Matériaux de Strasbourg (UMR7504), 23 rue du Loess, BP 34 67034 Strasbourg Cedex 2, France*

Table SI1. Ir content in Ir-SAC and Ir-NC, determined by ICP-OES, and N, C and H concentration in AC, and Ir-SAC, determined by CHNS.

Figure SI1. HAADF-STEM images of Ir-SAC and TEM images of Ir-NC with an average size of 1.3 nm.

Figure SI2. XANES spectra of Ir bulk (black), Ir-NC (red), Ir-SAC (blue) and IrO₂ (green) showing the difference in peak heights for these samples, and the parameters *a* and *b* used for the assessment of the oxidation state.

Figure SI3. EXAFS fitting of Ir-SAC before pre-treatment under He flow at 25°C (a, b) and after reaction under He flow at 25°C (c, d).

Figure SI4. XANES spectra (A), EXAFS signals (B) and related modulus of the Fourier Transform of the k²-weighed EXAFS signals (C) of the Ir-NC recorded at room temperature for the following states: initial (under air), initial under flow of H₂/He, after pre-treatment under H₂/He at 250 °C and after reaction at 200 °C. Examples of EXAFS fittings (D and E).

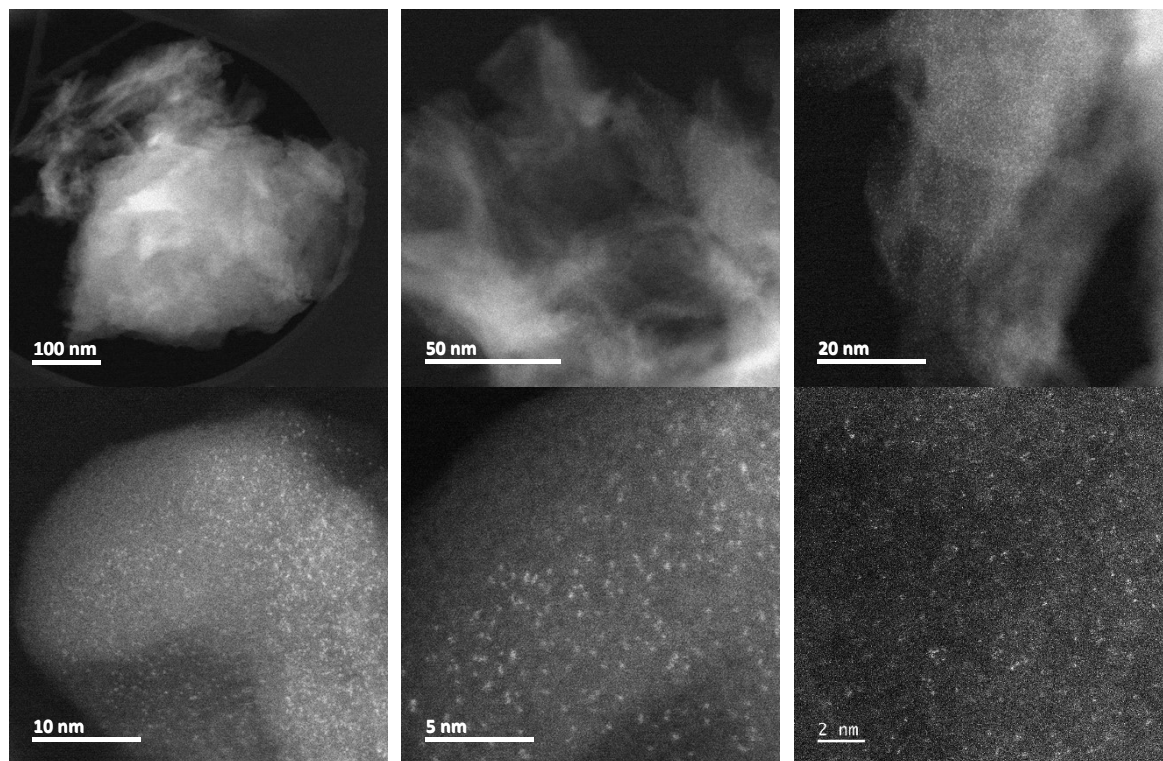
Figure SI5. Mass spectrometry monitoring of hydrocarbon reactant and products during the hydrogenation of butadiene on Ir-SAC and Ir-NC.

Figure SI6. Ex situ STEM-HAADF images of Ir-SAC as-prepared (A), after treatment under H₂/Ar flow at 250 °C (B) and 400 °C (C).

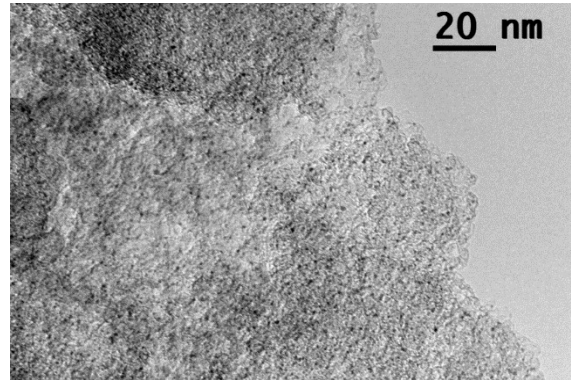
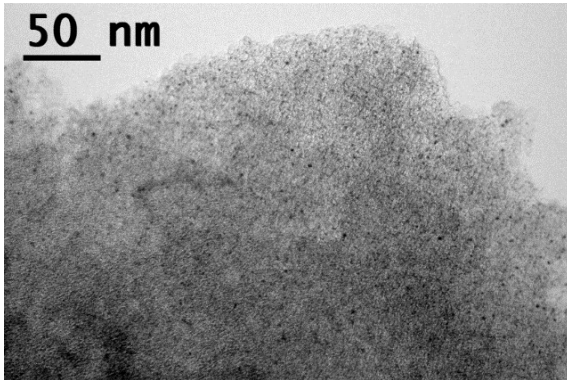
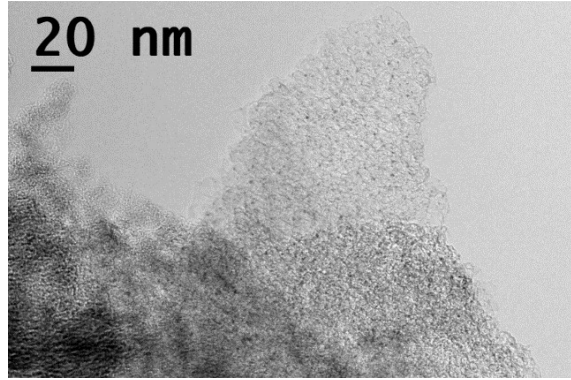
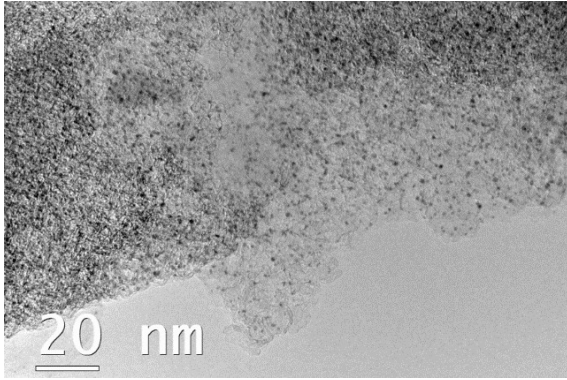
Table S11. Ir content in Ir-SAC and Ir-NC, determined by ICP-OES, and N, C and H concentration in AC, and Ir-SAC, determined by CHNS.

Sample	ICP-OES	CHNS		
	Metal content (wt. %)	N (wt. %)	C (wt. %)	H (wt. %)
AC	-	0.47 (± 0.08)	78.39 (± 0.81)	0.22 (± 0.04)
Ir-SAC	0.99 (± 0.01)	14.07 (± 0.15)	68.97 (± 0.11)	0.43 (± 0.03)
Ir-NC	3.70 (± 0.02)	-	-	-

Figure SI1. HAADF-STEM images of Ir-SAC and TEM images of Ir-NC with an average size of 1.3 nm.



Six HAADF-STEM images of Ir-SAC. No nanoparticles could be noticed in the low magnification images.



Four TEM image of Ir-NC. Well dispersed Ir nanoparticles are visible in these TEM images.

Figure S12. XANES spectra of Ir bulk (black), Ir-NC (red), Ir-SAC (blue) and IrO₂ (green) showing the difference in peak heights for these samples, and the parameters a and b used for the assessment of the oxidation state.

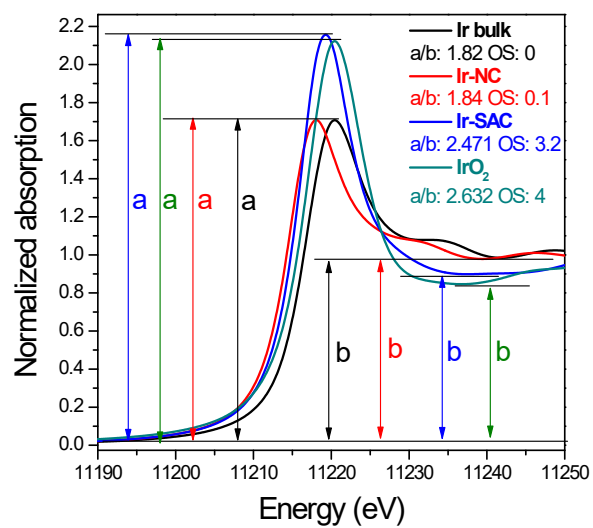


Figure SI3. EXAFS fitting of Ir-SAC before pre-treatment under He flow at 25°C (a, b) and after reaction under He flow at 25°C (c, d).

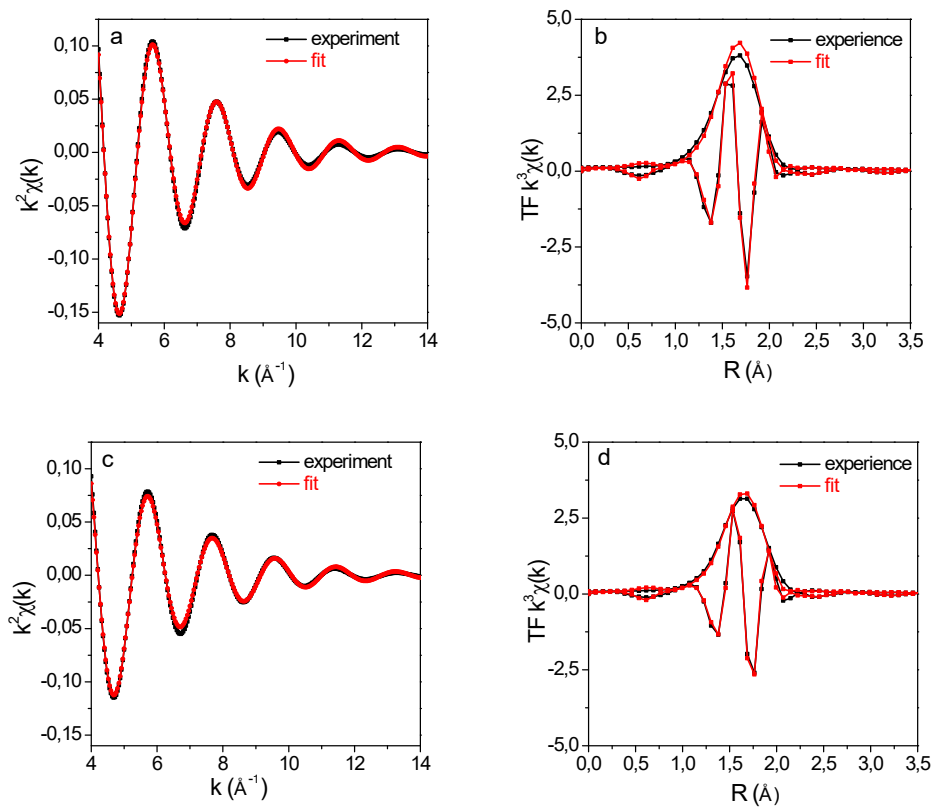
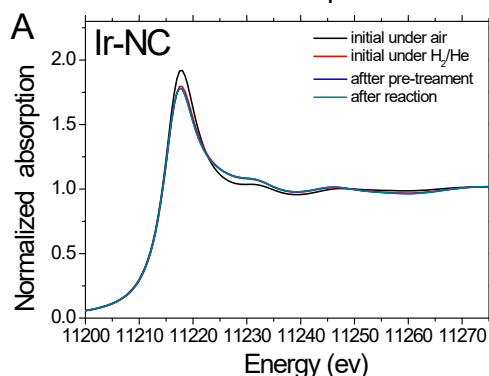
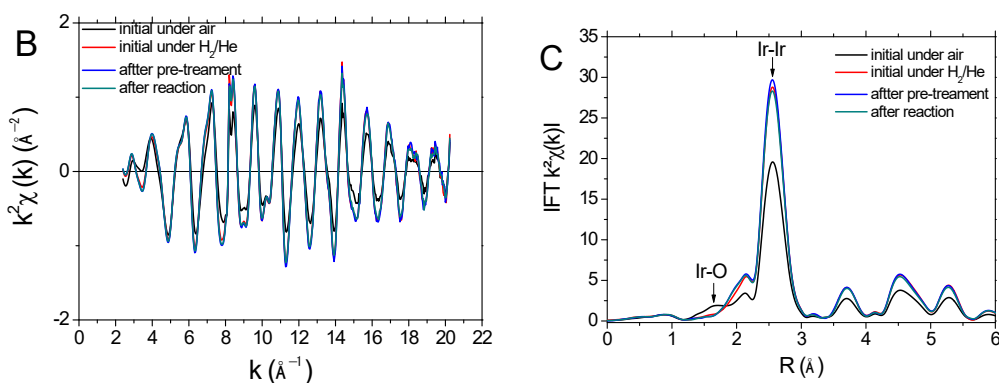


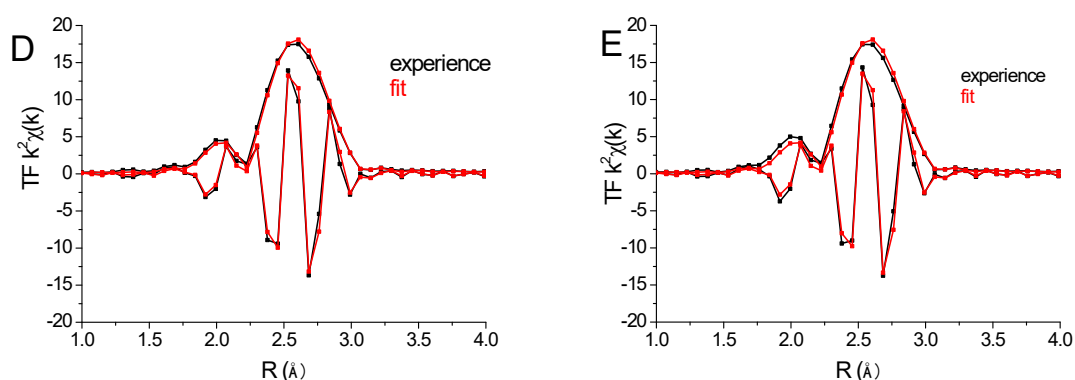
Figure SI4. XANES spectra (A), EXAFS signals (B) and related modulus of the Fourier Transform of the k^2 -weighted EXAFS signals (C) of the Ir-NC recorded at room temperature for the following states: initial (under air), initial under flow of H_2/He , after pre-treatment under H_2/He at 250 °C and after reaction at 200 °C. Examples of EXAFS fittings (D and E).



XANES spectra of the Ir-NC recorded at room temperature for the following states: initial (under air), initial under flow of H_2/He , after pre-treatment under H_2/He at 250 °C and after reaction at 200 °C.

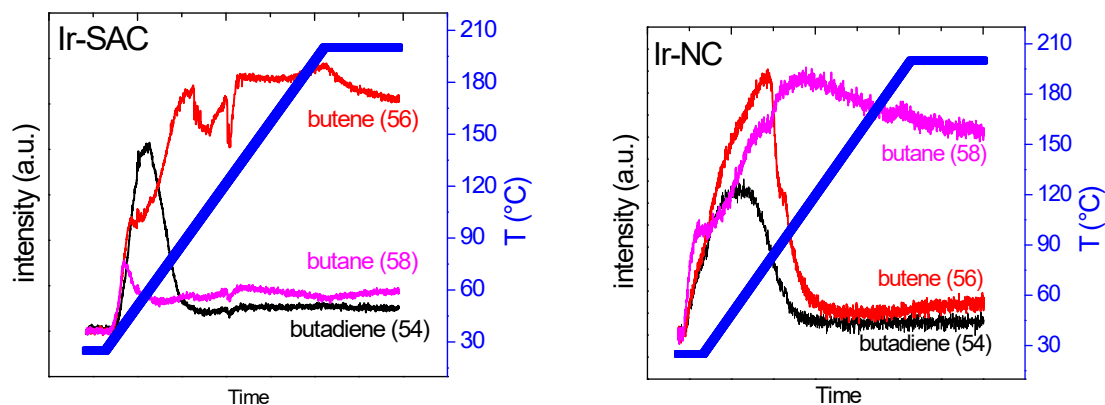


EXAFS spectra and related modulus of the Fourier Transform of the k^2 -weighted EXAFS signals recorded at room temperature for the Ir-NC for the following states: initial (under air), initial under flow of H_2/He , after pre-treatment under H_2/He at 250 °C and after reaction at 200 °C.



Examples of EXAFS fitting for Ir-NC initial under flow of H_2/He at room temperature (D) and after reaction at room temperature (E).

Figure SI5. Mass spectrometry monitoring of hydrocarbon reactant and products during the hydrogenation of butadiene on Ir-SAC and Ir-NC.



The gaseous product distributions during reaction of both Ir-SAC and Ir-NC were detected by mass spectroscopy during XAS experiments. The peaks of the fragments from butadiene, butene and butane in MS spectrum range from $m/z=15$ to $m/z=59$ and their product pools are very similar. After a careful selection, the pristine $m/z=54$, $m/z=56$ and $m/z=58$ signals were chosen to represent butadiene, butenes and butane during reaction, respectively, although they are not the principal peaks in the mass spectroscopy standard data (<https://webbook.nist.gov>).

Ir-SAC was highly active and selective to butenes while butane was the principal product for Ir-NC. The result is consistent with laboratory catalytic tests, confirming that *operando* XAS experiments were conducted in the same conditions.

Figure SI6. Ex situ STEM-HAADF images of Ir-SAC as-prepared (A), after treatment under H₂/Ar flow at 250 °C (B) and 400 °C (C).

